JACS
JOURNAL OF THE AMERICAN CHEMICAL SOCIETY

COMMUNICATION

pubs.acs.org/JACS

Delamination of Layered Zeolite Precursors under Mild Conditions: Synthesis of UCB-1 via Fluoride/Chloride Anion-Promoted Exfoliation

Isao Ogino,[†] Michael M. Nigra,[†] Son-Jong Hwang,[§] Jeong-Myeong Ha,[†,⊥] Thomas Rea,[‡] Stacey I. Zones,[*,†,‡] and Alexander Katz[*,†]

[†]Department of Chemical and Biomolecular Engineering, University of California at Berkeley, Berkeley, California 94720, United States

[‡]Chevron Energy Technology Company, Richmond, California 94804, United States

[§]Division of Chemistry and Chemical Engineering, California Institute of Technology, Pasadena, California 91125, United States

Supporting Information

ABSTRACT: New material UCB-1 is synthesized via the delamination of zeolite precursor MCM-22 (P) at pH 9 using an aqueous solution of cetyltrimethylammonium bromide, tetrabutylammonium fluoride, and tetrabutylammonium chloride at 353 K. Characterization by powder X-ray diffraction, transmission electron microscopy, and nitrogen physisorption at 77 K indicates the same degree of delamination in UCB-1 as previously reported for delaminated zeolite precursors, which require a pH of greater than 13.5 and sonication in order to achieve exfoliation. UCB-1 consists of a high degree of structural integrity via ^{29}Si MAS NMR and Fourier transform infrared spectroscopies, and no detectable formation of amorphous silica phase via transmission electron microscopy. Porosimetry measurements demonstrate a lack of hysteresis in the N_2 adsorption/desorption isotherms and macroporosity in UCB-1. The new method is generalizable to a variety of Si:Al ratios and leads to delaminated zeolite precursor materials lacking amorphization.

The emergence of a new class of catalysts consisting of exfoliated zeolite precursors expands the range of reactions that zeolites catalyze by providing access for larger reactant molecules.[1−4] ITQ-2 in particular represents the first example of such a material, and consists of pores derived from the zeolite precursor material MCM-22(P), which are embedded within thin, accessible sheets and enable shape-selective catalysis.[5−9] To date, the synthesis of exfoliated zeolite precursors has required a high-pH medium during precursor material swelling, typically in the pH range of 13.5−13.8.[10−12] On the basis of the high solubility of silica in such a basic aqueous solution, hypotheses of partial amorphization of the zeolite layers during delamination have been invoked.[10,11,13] This has motivated the search for milder conditions for delamination. While there has been notable success in decreasing the temperature from 353 K to room temperature during swelling of MCM-22 (P), it has been difficult to achieve delamination under these milder conditions, since the material reverts back to the zeolite precursor after acidification of the swollen sample.[11] Here, in this manuscript, we demonstrate the synthesis of UCB-1, which results from MCM-22 (P) exfoliation using a combination of tetrabutylammonium fluoride and chloride surfactants at pH 9 in aqueous solution, and is isolated in an aluminosilicate yield of 90% (versus ∼75% aluminosilicate yield for ITQ-2 synthesis in our hands). We demonstrate unique morphology and high structural integrity of UCB-1, which are characterized by ^{29}Si MAS NMR spectroscopy, transmission electron microscopy (TEM), and porosimetry.

Delamination of layered zeolite precursors by the new method is guided by viewing exfoliation from the perspective of being a chemical deprotection process, involving breaking of Si−O and Al−O bonds in the interlayer region. Our approach uses fluoride anion because it is an established reagent for the deprotection of silyl ethers[14] and is known to form strong interactions to Si(IV) cations.[15,16] In addition, chloride is used because it is known to be the most aggressive anion for corroding anodized aluminum among a list of 12 investigated anions that include all four common halides.[17] We therefore hypothesized that delamination can be conducted using an aqueous mixture of fluoride and chloride anions. Thus, treatment of MCM-22 (P) at 353 K for 16 h using cetyltrimethylammonium bromide, tetrabutylammonium fluoride, and tetrabutylammonium chloride at a mild pH of 9 (typically associated with fluoride syntheses of zeolites[18]) results in delamination. These conditions correspond to the same temperature and duration used under the conventional high-pH delamination method but, in contrast, crucially lack the requirement of sonication. After acidification of the slurry to pH 2, the delaminated zeolite precursor UCB-1 is collected via centrifugation.

Powder X-ray diffraction (PXRD) of as-made UCB-1 data are shown alongside data for zeolites MCM-22 (P) (Figure 1, pattern A) and ITQ-2 (pattern B), which match literature data (see the Supporting Information for details).[1,6,12]

PXRD of as-made UCB-1 in Figure 1C demonstrates a powder pattern similar to that of ITQ-2 zeolite. The 001 (3.3°, ∼27 Å) and 002 (6.7°, ∼13 Å) peaks are significantly diminished in intensity; however, the 310 (26°) peak has a stronger intensity than for material ITQ-2. This suggests a greater degree of long-range order in the direction parallel to the sheet for the material synthesized by the fluoride/chloride delamination method.

Whereas TEM images of MCM-22 (P) show lamellar assemblies consisting of rectilinear sheets (Figure S1A and B in the Supporting Information), images of UCB-1 clearly show curved layers (Figure S1C and D in the Supporting Information), which lack long-range order. Single layers of 2.5 nm thickness

Received: December 10, 2010
Published: February 22, 2011

dx.doi.org/10.1021/ja111147z | J. Am. Chem. Soc. 2011, 133, 3288–3291

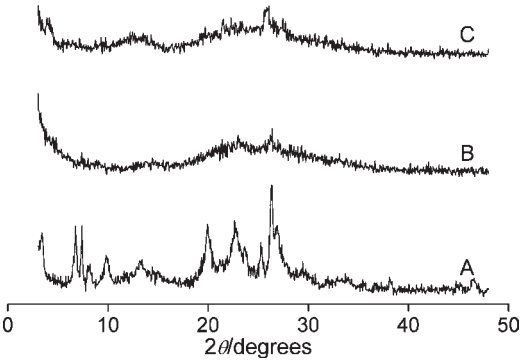

Figure 1. Powder X-ray diffraction patterns characterizing as-made zeolites (A) MCM-22 (P), (B) ITQ-2, and (C) UCB-1.

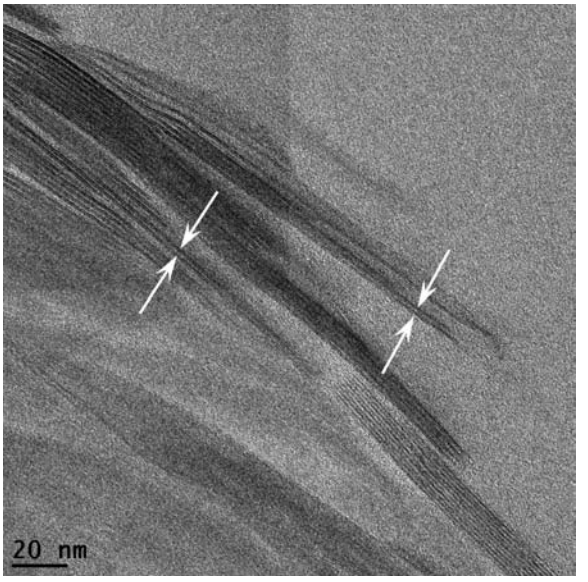

Figure 2. TEM image characterizing as-made UCB-1. The arrows indicate single-layers.

are evident in Figure 2 (see also Figure S2 in the Supporting Information).

^{29}Si MAS and CP MAS NMR spectra in Figures 3 and 4 further compare MCM-22 (P) with as-made materials ITQ-2 and UCB-1. The well-resolved resonances in the Q^4 region ($-105 < \delta < -120$ ppm) and entire absence of Q^2 resonances for the spectrum in Figure 3C relative to Figure 3B reflect a higher degree of structural order for UCB-1 compared with ITQ-2.

The observed breadth of the Q^4 region and the appearance of downfield Q^2 resonances (~ -91 ppm) in Figures 3B and 4A for as-made ITQ-2 are consistent with amorphization of the zeolite precursor material. Fourier-transform infrared (FTIR) spectra (Figure S3 in the Supporting Information) of both as-made and calcined UCB-1 exhibit a well-resolved band at 563 cm^{-1}. This distinct band corresponds to pentasil rings in the framework[19] and is also similarly evident in MCM-22(P). The significantly diminished intensity of this band in the spectrum of ITQ-2[1] is presumably the result of amorphization.[10,11,13] ^{27}Al MAS NMR spectroscopy (Figure S4 in the Supporting Information) demonstrates retention of tetrahedral aluminum at 50−60 ppm and no octahedral aluminum at around 0 ppm in as-made UCB-1.[20]

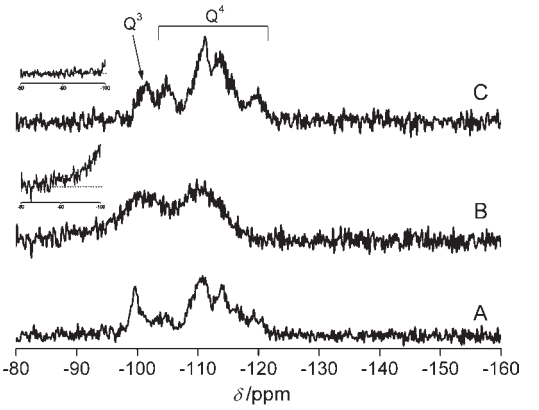

Figure 3. ^{29}Si MAS NMR data characterizing (A) MCM-22 (P), (B) as-made ITQ-2, (C) as-made UCB-1. Insets: Magnification of spectra in the range between −80 and −100 ppm.

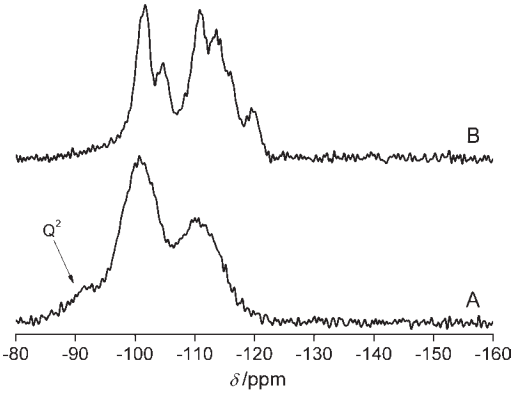

Figure 4. ^{29}Si CP MAS NMR data characterizing (A) as-made ITQ-2 and (B) as-made UCB-1. The spinning rate of the sample was 8 kHz, and contact time for cross-polarization was 2.0 ms.

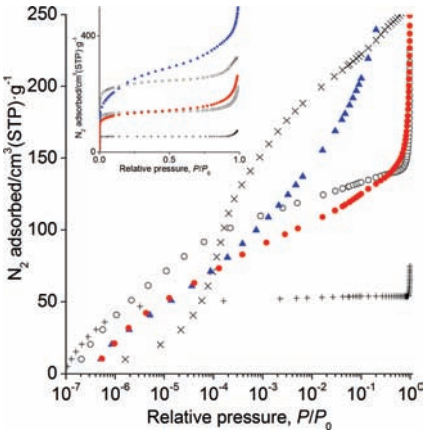

Figure 5. N_2 adsorption isotherms characterizing the following zeolites in a semilogarithmic scale: (○) MCM-22 zeolite, (▲ blue) ITQ-2 zeolite, (● red) UCB-1, (×) USY zeolite, and (+) TON zeolite. The inset shows the same data in a linear scale.

Nitrogen physisorption isotherms at 77 K of calcined materials UCB-1 and ITQ-2, as well as calcined zeolites MCM-22,[21] TON,[22] and ultrastable HY (USY), are shown in Figure 5. The latter three are included as controls to elucidate where in the isotherm rings of a certain size physisorb nitrogen. Zeolite TON consists of only

dx.doi.org/10.1021/ja111147z |J. Am. Chem. Soc. 2011, 133, 3288–3291

10-membered-ring (MR) channels and shows pore filling of these channels starting at a relative pressure P/P_o of 10^{-7}. Zeolite USY consists of 12-MR windows and large (~13 Å) supercages, and shows pore filling of these pores at a relative pressure in the range of $10^{-5} < P/P_o < 10^{-4}$.

As a reference point, calcined zeolite MCM-22 consists of two independent 10-MR pore channels and 12-MR supercages,[21] with one of the 10-MR pore channel systems running through intralayers and the other through interlayers. Therefore, the delamination of MCM-22 (P) and its subsequent calcination is expected to form a material that retains 10-MR pore channels within each layer, while the other 10-MR pore channel is expected to be significantly reduced relative to calcined MCM-22 zeolite.[23] These expectations are indeed supported by a comparison of N_2 physisorption data for calcined MCM-22 and ITQ-2 in Figure 5. At a relative pressure of approximately $10^{-7} < P/P_o < 10^{-4}$, the total uptake of nitrogen into ITQ-2 is lower than that for MCM-22, which is consistent with loss of 10-MR during the delamination process. The isotherm for UCB-1 in Figure 5 essentially overlaps the isotherm for ITQ-2 in the region $10^{-7} < P/P_o < 10^{-4}$, which indicates that both materials have similar amounts of 10-MR channels (Table S1 in the Supporting Information). This in turn requires that the degree of delamination for both materials is similar. However, the significantly diminished uptake of UCB-1 for relative pressures P/P_o greater than 10^{-4} means that ITQ-2 consists of larger micropores and mesopores, which presumably originate from amorphous silica and are responsible for the hysteresis observed in the adsorption/desorption branches of the nitrogen physisorption isotherm of ITQ-2 (Figure S5 in the Supporting Information). This hysteresis is entirely absent in the corresponding isotherms of UCB-1 (see Figure S5 in Supporting Information). Mesoporosity in ITQ-2 and lack thereof in UCB-1 are additionally confirmed via TEM (Figure S6 in the Supporting Information).[10]

The structural integrity of layers in UCB-1 is evident in the large length scale of macroporosity via mercury porosimetry (Figure S7 in the Supporting Information). The average macropore diameter of 350 nm in UCB-1 is almost the same as the 0.5−1 μm microcrystalline diameter of the MCM-22 (P) used in the synthesis of UCB-1. Considering the curvature incorporated into UCB-1 layers upon delamination (vide supra), this is consistent with minimal intralayer fragmentation. TEM of calcined UCB-1 also demonstrates this macroporosity, which is formed between stacks of sheets. In contrast, though both materials are synthesized from the same layered zeolite precursor, the macropore diameter of calcined ITQ-2 is significantly smaller than that for UCB-1. This is consistent with fragmentation of ITQ-2 layers during the higher pH conventional delamination process.

When delamination is attempted using only fluoride in the absence of chloride, only partial delamination results. This is clearly demonstrated by the strong 001 and 002 peaks at 3.3° (d-spacing of ~27 Å) and 6.7° (d-spacing of ~13 Å) in Figure 6B. These features in the powder X-ray diffraction pattern indicate retention of layer stacking after delamination in the absence of chloride. The essential role of chloride demonstrated by the data above could be due to its ability to break Al−O bonds in the interlayer region, as demonstrated by its corrosivity of oxidized aluminum (vide supra). However, the crucial role of hybrid organic−inorganic self-assembly should also not be underestimated. There is much precedent for chloride-specific anion binding effects in the noncovalent stabilization of interfaces in general. In particular, chloride has been shown by classical Monte Carlo simulations to interact directly with Al−OH functionality in γ-alumina.[24] Furthermore, zeta potential measurements show chloride to be unique among other investigated halides consisting of bromide and iodide, in that chloride is able to specifically adsorb on an α-alumina surface.[25] Thus, chloride could also play an important role in stabilizing the supramolecular assembly that results during delamination by providing for required noncovalent interactions and space filling.[26]

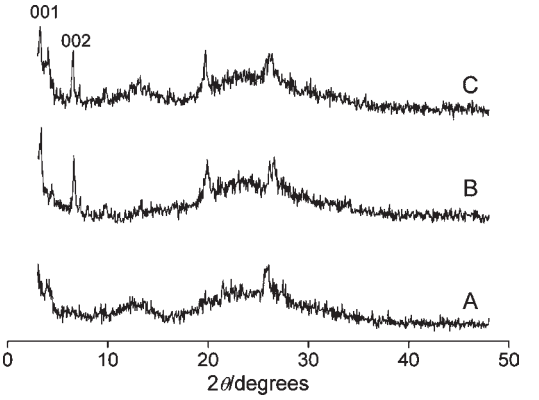

Figure 6. Powder X-ray diffraction patterns characterizing (A) as-made UCB-1, and MCM-22(P) (Si:Al ratio of 50) delaminated by the same method used for UCB-1, except in the absence of either (B) chloride or (C) fluoride.

Fluoride is also a necessary component for delamination because using only chloride in the absence of fluoride results in partial delamination as well. This is demonstrated by Figure 6C, which is similar to the powder X-ray diffraction pattern in Figure 6B. We hypothesize that coordination of fluoride to Si is critical for at least the partial replacement of Si−O with Si−F functionality in the interlayer region during MCM-22(P) delamination. Support for fluoride coordination to Si is contained in the ^{19}F NMR spectrum of as-made UCB-1 (Figure S8 in the Supporting Information), which exhibits a resonance at −128.6 ppm that is attributable to SiF_6^{2-}.[27]

The mild pH and lack of sonication used for UCB-1 synthesis are directly comparable with those used to synthesize ITQ-2, by applying both treatments to calcined zeolite MCM-22 as an aluminosilicate model. The treatment of calcined MCM-22 under UCB-1 synthesis conditions leads to a product with an intense powder pattern resembling parent MCM-22 (Figure S9 in the Supporting Information). However, treatment of calcined MCM-22 under ITQ-2 synthesis conditions leads to decreased zeolite crystallinity as evidenced by intense amorphous features and weaker overall peak intensity in the PXRD pattern (Figure S10 in Supporting Information). This comparison demonstrates the milder nature of UCB-1 versus ITQ-2 synthetic conditions on the aluminosilicate framework.

While the results above have been demonstrated by using a MCM-22 (P) with a Si:Al ratio of 50, similar degrees of delamination via PXRD are achieved in materials having a Si:Al ratio of 20 (PXRD pattern is shown in Figure S11 in the Supporting Information). This has been performed using similar conditions to those reported here using the fluoride/chloride method, except that a swelling time of 3 d rather than 16 h is used.

In summary, the fluoride/chloride method presented here successfully delaminates layered zeolite precursors at a pH of 9 in aqueous solution and, as such, presents the mildest known

method for the delamination of zeolite precursor materials. We anticipate that the method can be readily generalized to other layered zeolite precursors consisting of a variety of Si:Al ratios.

■ ASSOCIATED CONTENT

Supporting Information. Experimental procedures, TEM images, ^{27}Al MAS NMR spectra, ^{19}F MAS NMR spectra, FTIR spectra, N_2 physisorption, and mercury porosimetric data. This material is available free of charge via the Internet at http://pubs.acs.org/page/copyright/journals/index.html.

■ AUTHOR INFORMATION

Corresponding Author

sizo@chevron.com; askatz@berkeley.edu

Present Addresses

[⊥]Korea Institute of Science and Technology, Seoul 136-791, Republic of Korea

■ ACKNOWLEDGMENT

We acknowledge Prof. Enrique Iglesia for generosity in resources and for useful discussion about porosity in these types of materials, Dr. Alexander Kuperman at Chevron for helpful discussion regarding delamination mechanism, and Dr. Anja Rumplecker for assistance in the syntheses of MCM-22 (P) and ITQ-2 zeolites. We are grateful to the Management and Transfer of Hydrogen via Catalysis Program funded by Chevron Corporation for financial support. The NMR facility at Caltech is supported by the National Science Foundation (NSF) under the Grant Number 9724240 and partially supported by the MRSEC program of NSF under Award Number DMR-520565.

■ REFERENCES

(1) Corma, A.; Fornés, V.; Pergher, S. B.; Maesen, T. L. M.; Buglass, J. G. *Nature* **1998**, *396*, 353–356.
(2) Corma, A.; Díaz, U.; Domíne, M. E.; Fornés, V. *J. Am. Chem. Soc.* **2000**, *122*, 2804–2809.
(3) Corma, A.; Díaz, U.; Domíne, M. E.; Fornés, V. *Angew. Chem., Int. Ed.* **2000**, *39*, 1499–1501.
(4) Corma, A.; Fornés, V.; Díaz, U. *Chem. Commun.* **2001**, 2642–2643.
(5) Aguilar, J.; Pergher, S. B. C.; Detoni, C.; Corma, A.; Melo, F. V.; Sastre, E. *Catal. Today* **2008**, *133*, 667–672.
(6) Corma, A.; Fornés, V.; Martínez-Triguero, J.; Pergher, S. B. *J. Catal.* **1999**, *186*, 57–63.
(7) Rodríguez, I.; Climent, M. J.; Iborra, S.; Fornés, V.; Corma, A. *J. Catal.* **2000**, *192*, 441–447.
(8) Botella, P.; Corma, A.; Iborra, S.; Montón, R.; Rodríguez, I.; Costa, V. *J. Catal.* **2007**, *250*, 161–170.
(9) Corma, A.; García, H.; Miralles, J. *Microporous Mesoporous Mater.* **2001**, *43*, 161–169.
(10) Schenkel, R.; Barth, J. O.; Kornatowski, J.; Lercher, J. *Stud. Surf. Sci. Catal.* **2002**, *142A*, 69–72.
(11) Maheshwari, S.; Jordan, E.; Kumar, S.; Bates, F. S.; Penn, R. L.; Shantz, D. F.; Tsapatsis, M. *J. Am. Chem. Soc.* **2008**, *130*, 1507–1516.
(12) Roth, W. J.; Vartuli, J. C. *Stud. Surf. Sci. Catal.* **2002**, *141*, 273–279.
(13) Wu, P.; Nuntasri, D.; Ruan, J. F.; Liu, Y. M.; He, M. Y.; Fan, W. B.; Terasaki, O.; Tatsumi, T. *J. Phys. Chem. B* **2004**, *108*, 19126–19131.
(14) Wuts, P. G. M; Greene, T. W. *Greene's Protective Groups in Organic Synthesis*; Wiley-Interscience: New York, 2007.
(15) Koller, H.; Wölker, A.; Eckert, H.; Panz, C.; Behrens, P. *Angew. Chem., Int. Ed.* **1997**, *36*, 2823–2825.
(16) Koller, H.; Wölker, A.; Villaescusa, L. A.; Díaz-Cabañas, M. J.; Valencia, S.; Camblor, M. A. *J. Am. Chem. Soc.* **1999**, *121*, 3368–3376.
(17) Trompette, J. L.; Arurault, L.; Fontorbes, S.; Massot, L. *Electrochim. Acta* **2010**, *55*, 2901.
(18) Camblor, M. A.; Corma, A.; Valencia, S. *J. Chem. Soc., Chem. Commun.* **1996**, 2365–2366.
(19) Corma, A.; Corell, C.; Pérez-Pariente, J.; Guil, J. M.; Guil-López, R.; Nicolopoulos, S.; Calbet, J. G.; Vallet-Regi, M. *Zeolites* **1996**, *16*, 7.
(20) Lawton, S. L.; Fung, A. S.; Kennedy, G. J.; Alemany, L. B.; Chang, C. D.; Hatzikos, G. H.; Lissy, D. N.; Rubin, M. K.; Timken, H. K. C.; Steuernagel, S.; Woessner, D. E. *J. Phys. Chem.* **1996**, *100*, 3788.
(21) Leonowicz, M. E.; Lawton, J. A.; Lawton, S. L.; Rubin, M. K. *Science* **1994**, *264*, 1910–1913.
(22) Barri, S. A. I.; Smith, G. W.; White, D.; Young, D. *Nature* **1984**, *312*, 533–534.
(23) Corma, A.; Fornés, V.; Guil, J. M.; Pergher, S.; Maesen, T. L. M.; Buglass, J. G. *Microporous Mesoporous Mater.* **2000**, *38*, 301–309.
(24) Criscenti, L. J.; Cygan, R. T.; Kooser, A. S.; Moffat, H. K. *Chem. Mater.* **2008**, *20*, 4682–4693.
(25) Das, M. R.; Borah, J. M.; Kunz, W.; Ninham, B. W.; Mahiuddin, S. *J. Colloid Interface Sci.* **2010**, *344*, 482.
(26) Ninham, B. W.; Yaminsky, V. *Langmuir* **1997**, *13*, 2097.
(27) Camblor, M. A.; Barrett, P. A.; Díaz-Cabañas, M. J.; Villaescusa, L. A.; Puche, M.; Boix, T.; Pérez, E.; Koller, H. *Microporous Mesoporous Mater.* **2001**, *48*, 11–22.